Journal of Data Acquisition and Processing
ISSN: 1004-9037
https://sjcjycl.cn/
DOI: 10.5281/zenodo.7765777

DESIGN AND ANALYSIS OF WAVY PROFILE ON THREE DIMENSIONAL AIRCRAFT WING

[1]V.Jaya kumar, [2]M.Gunashree, [3]Balaji, H [4]Y. Abinesh
[1] Students, [2] Assistant Professor.
[1,2] Department of Aeronautical Engineering,
[1] Assistant Professor, Tagore Engineering College, Chennai, India [2]Student, GKM College of Engineering and Technology, Chennai, India [3] Assistant Professor, Tagore Engineering College, Chennai, India 4Student, Tagore Engineering College, Chennai, India
[1] jaikumar.v16@gmail.com [2] shreesri9899@gmail.com,[3] balaji.hk007@gmail.com
[4]abineshy102003@gmail.com

ABSTRACT
The wavy taper wings configuration showed fascinating result in current studies. The effect of flow properties over a finite wing causes difference performance due to tubercle and also
TR Taper Ratio
AR Aspect Ratio
V Velocity
analyzing the influence of flow in wavy profile λ on three dimensional aircraft wings at low velocity. A software analysis was carried out to C
change the geometric parameter of the wing with taper ratio and amplitude. The wings were
Wavelength
In the last few years, the flow control designed by amplitude method and using CATIA. The flow variations results showed that the configurations to be high vulnerable effect of the wavy profile.as it gives to increase in lift co- efficient. The CFD analysis are done by using FLUENT. This analysis is conducted for the models in with and without tubercles. All wing models had a basic NACA0020 airfoil and also consider the tubercle geometry with amplitude of 0.03c and the wavelength of 0.11c. The aim of this analysis is to find the drag and lift force at velocity 30.6m/s for all models and these results are compared with the normal wings. Flow visualization analysis gives better results and to understand the wavy profile effect in the leading edge of the wing.

NOMENCLATURE:
A Amplitude
AOA Angle of Attack
method of leading edge tubercles has enticed increasing and improving analyses to explore the potential obtain in aerodynamic and hydrodynamic performance for designs such as control surface, aircraft wings, tidal turbines etc. It has been conjecture that humpback whales position the wavy distributed along their leading edge to achieve maneuverability as rolls and also loops. At low velocity regime aerodynamic performance is determined by the behavior of the laminar boundary layer separation. The aircraft showing can be worsening even at low AOA. Since Micro Aerial Vehicles (MAV) and Unmanned Aerial Vehicles (UAV) at low velocity rule and

they also have requirements of the performance. Recently, the airfoil phenomena have been analyzed at low velocity in order to upgrade aerodynamic showing in this particular rule.

In the 2000's, scientists to investigate the sinusoidal leadingedge airfoils.

Cl_{MAX}

Maximum lift Co-efficient

Miklosovicetal1 (2004), incite on the wavy of the humpback flipper execute the studies of

Cd_{MAX} Maximum Drag Co-efficient αstall Stall angle

sinusoidal wavy leading edge phenomena and then showed a potential obtain in hydrodynamic and aerodynamic well ordered. (fig 1).

Miklosovicetal2 (2007) this wavy leading edge effect in the two-dimensional flow (full wing span) furthermore the three- dimensional flow (partial wing span). NACA 0020 symmetric airfoil was also performed and tested in the wind tunnel for Reynolds number range between 274000 and 277000. Joharietal3 (2007) execute test with full wing span.

Fig 1. A humpback whale and the outstanding wavy on the leading edge Boston, Massachusetts, USA 2019 https://unsplash.com/photos/lwACYK8ScmA/info

Stanway5 (2008) test a model in a wind tunnel and that model is similar to Miklosovicetal1(2004) and also managing the symmetric profile NACA 0020 at Reynolds number range from 44000 to 120000. The stall angle behavior is gradual. The stall angle attain lag in all condition of Reynolds number. It is compared to the normal airfoil. This behavior is similar to Miklosovicetal1 (2004) results.

Miklosovicetal2 (2007) the efforts of tubercle leading edge on aerodynamic performance for full and partial wing spans are really dissimilar though the flow method give rise to by the wavy is mostly same. At pre stall conditions, the consequence for the both models show similar behavior compare to the normal wing configuration at lower angle of attack. For high angle of attack up to the stall and also the full span wing model shows that the noticed aerodynamic changes with become less lift. Regarding the partial wing span model only a small fine appear up to the stall angle. This configuration overcoming the lift of the normal airfoil. The post stall rule, the full span wing model presents minimum stall performance and compared to the partial span wing. (fig 2)

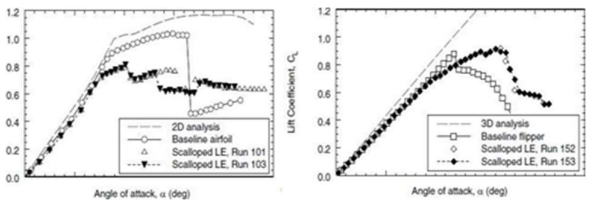

Fig 2. Three dimensional effects on the wavy leading edge performance Miklosovicetal2 (2007)

In spite of tubercles showing dissimilar between full and partial wing consequence are justified by the merging of different of effects. Stanway5 (2008) said that the Reynolds number have a bump on tubercle leading edge performance as consequence of changes in stall.

The tubercle on the flipper outwards sections prevent the propagation of the leading edge stall with consider to the root. In the inboard sections the wavy generates vortices.

The wavy effects are dissimilar for inwards and outwards regions and this impacts are dependent on Reynolds number taper ratio and aspect ratio as pointed out by Miklosovicetal2 (2007).

Hansen6(2010), To differentiate the feasible advantage of the Reynolds number impacts those arising from the three dimensional of the wing. It appraised various wavy leading edge geometries for both wing models with symmetric airfoil NACA 0021 without sweep nor taper. The tests are performed at a Reynolds number of 120000 for various wavy geometric specification. It was noted that the wavy leading edge showing for both wing models are same in comparison with consequences from Miklosovicetal2 (2007). Both wing models are the stupendous configuration was reached by the wavy leading edge design with the small amplitude and shortest wavelength. Hansen7(2010) suggest that the tubercle leading edge could be rising the performance of the wings. The taper wing owing to the fact these geometry parameters carry notable more span wise flow.

Custodioetal8(2012) carried out the experiment and also study the full span wing effects on tubercle leading edge performance. Experimentally both wing models with NACA 634021 airfoils were conducted. Four different planform geometries were used: both span

rectangular wing, un-swept wing with aspect ratio of 2.15 and swept wing with (AR=2.0, Λ=260), and a model represented of a humpback whales flipper (AR=4.43). The consequence presents an advancement in the aerodynamic showing for the tubercle leading edge caused by the wing's three dimensionality impacts at post stall rule. The maximum coefficient of lift increase for full span wing configurations and compared to infinite wing.

Bolzonetetal9(2014) explored tests, the impacts of the wavy profile on swept tapered wing for low angle of attack at Re=200000. The wavy leading edge design is decrease lift and drag 4-6% and by 7-9% as respectively. The consequences in an increase of 3% in the maximum lift to drag ratio.

Abrantesetal11(2017) conducted a experiments occurs aerodynamic forces and visualization at Re=200000 and 80000 on four full wing span models with dissimilar planform parameters with difference taper ratio and swept angle. A wavy profile geometry of A=0.03c; λ=0.11c was selected based on the consequence of Depaulaetal12 and it is used to along the whole span. The force consequence for RE=200000 shows a lag in lift feature for the non-swept wing models. An increase of about 20% in lift co- efficient value was observed and noted for the swept and swept tapered wing. In the cases, drag co-efficient is only slightly increase at small angle of attack was detected. At low Re= 80000 all wing models are showed an increase in lift co-efficient and the stall behavior is also improvement.

Wei et al 13(2018) carried out an experiments at Reynolds number 220000 for a wavy tapered swept wing sweep angle of 300 and taper ratio=0.33. The wing design with SD7032 airfoil

profile. The wavy geometry specification A=0.12c and λ=0. 05c.The force consequence didn't increase in lift co-efficient and the stall behavior for tubercle design indicated better showing. Wavywing flow pattern indicate the very highly complexed surface vortex show surface at modest angle of attack.

Advancement in aerodynamics performance were noticed only in tapered wings for the observed and studies the research paper Abrantesetal11 (2017), the important purpose of this study is to analysis the impact of the wings models three dimensional flow on the tubercle leading edge at low velocity by varying the wing specification. The analysis was carried out varying amplitude for awing area in order to notice the impacts of these specification on

wavy leading edge when a wing area is considered for an aircraft design. All wing models had a basic NACA0020 airfoil and also consider the tubercle geometry with an amplitude of 0.03c and the wavelength of 0.11c. The aim of this analysis is to find the drag and lift force at velocity 30.6m/s for all models and these results are compared with the smooth or normal wings. Flow visualization gives better results.

ll. EXPERIMENTAL METHODOLOGY

To carry out the wings, each wing models are designed in smooth and wavy configuration. The wing models are designed by the following geometry parameter present in Table 1. The specific geometry is (A=0.03c; λ = 0.11c).

Table 1. Geometric parameters of the wing models

Model	**Designation**	**Amplitude (A=0.03c)**
Smooth Tapered 3D	ST 3D	0
Wavy Tapered 3D	WT 3D	½th of the distance of semi wing
Wavy Tapered3 D	WT 3D	¾th of the distance of semi wing

The smooth and wavy wing models were designed by using the airfoils with the help of CATIA, this software is one of the tool of computer

-aided design (CAD). But the wavy wing has different chord lengths by using amplitude method. The co-ordinate points are imported by using excel. A sinusoidal path is defined by wavy geometry. The following wing models are designed by using CATIA:

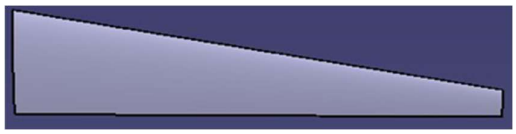

Fig 3(a) Smooth Tapered wing

Fig 3(b) Wavy Tapered wing (½th of the distance of semi wing)

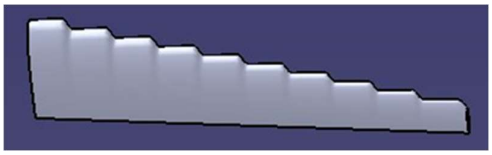

Fig 3(c) Wavy Tapered wing (¾th of the distance of semi wing)

The wing models are analyzed by using ANSYS FLUENT. The models are imported to the ansys and then create a boundary condition. The maximum velocity at 30.6m/s is used to analyze the models. The configurations were tested at low velocity. The velocity value is taken out by the Abrantes et al11 (2017). It measures the lift and drag forces were observed and obtained by using this software. During the performance of the wing and also create a different angle of attack then note a value of lift and drag forces.

III.ANALYSIS

A. Pressure and Velocity Distribution

A.1 Normal Taper Semi Wing: A.1.1ATAOA 6 DEGREE:

At angle of attack 6 degree in the smooth tapered wing, flow visualization, pressure and velocity distribution of a semi wingspan. (Fig.A
1.1 a-b-c).

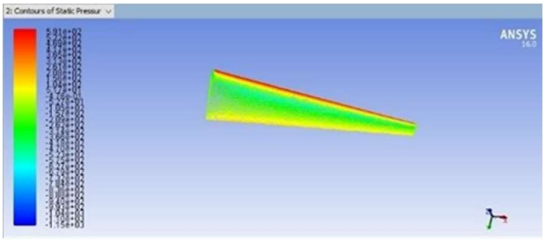

Fig A.1.1(a): pressure distribution at 6 degrees of AOA

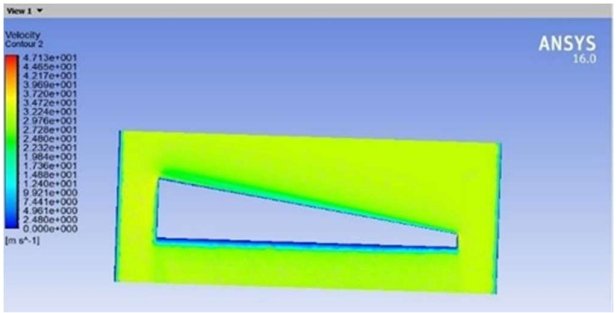

Fig. A.1.1(b): flow visualization at 6 degrees of AOA

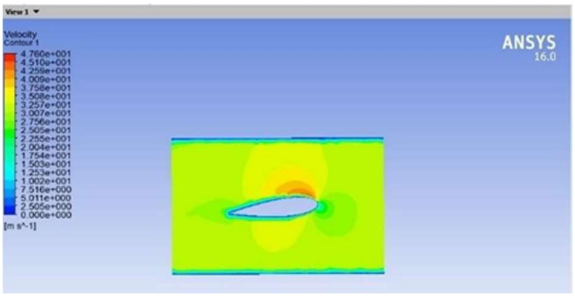

Fig. A.1.1(c): velocity distribution at 6 degrees of AOA

A.1.2 AT AOA 12 DEGREE:

At 12 degrees of Angle of attack in the smooth tapered wing, flow visualization, pressure and velocity distribution of a semi wingspan (Fig.A.1.2. a-b-c).

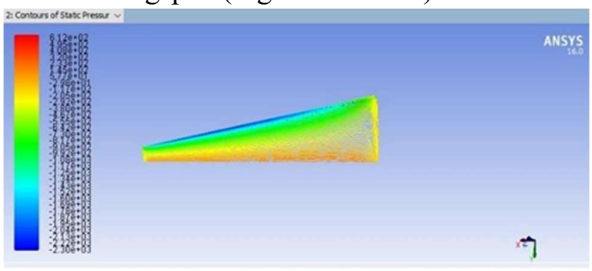

Fig.A.1.2 (a): pressure distribution at 12 degree of AOA

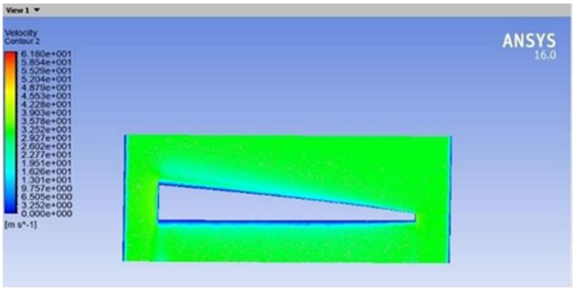

Fig.A.1.2 b): flow visualization at 12 degree of AOA

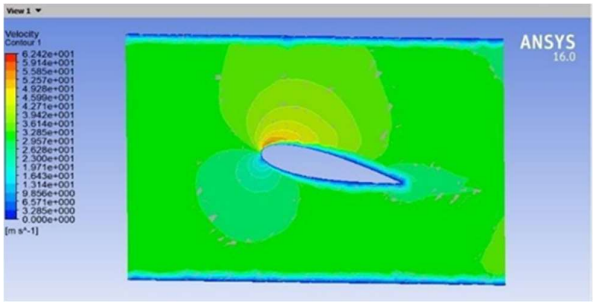

Fig A.1.2(b): velocity distribution at 12 degree of AOA

A.1.3 AT AOA 18 DEGREE:

At 18 degrees of Angle of attack in the smooth tapered wing, flow visualization, pressure and velocity distribution of a semi wingspan (Fig.A.1.3. a-b-c).

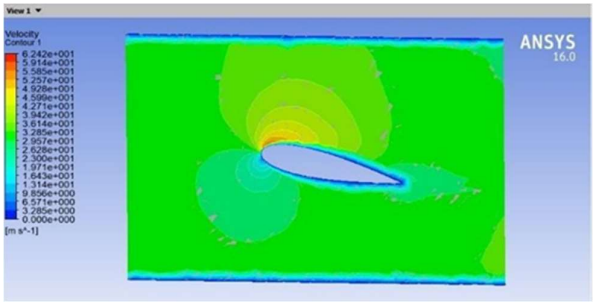

Fig. A.1.3 (a): pressure distribution at 18 degrees of AOA

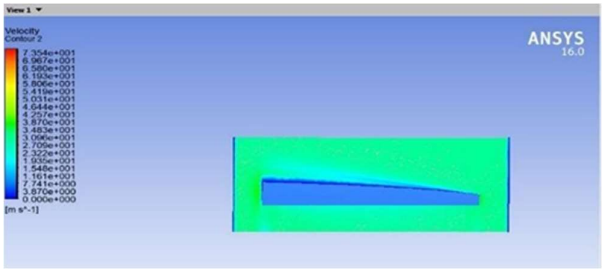

Fig. A.1.3(b): flow visualization at 18 degrees of AOA

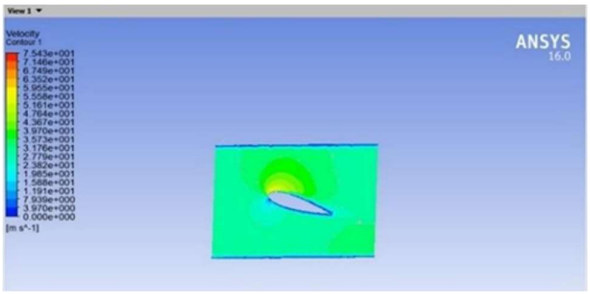

Fig.A.1.3(b): velocity distribution at 18 degrees of AOA

A.2

Half of the Distance Of Wavy Taper Semi Wing:

A.2.1 AT AOA 6 DEGREE:

At angle of attack 6 degree in the wavy wing design. The characteristic of flow over the entire wing span. However, observed the tubercle performance of the wing by the following figure. A flow visualization, pressure and velocity distribution of a semi wingspan (Fig A.2.1.a-b-c).

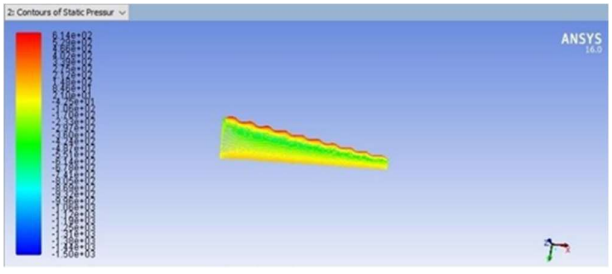

Fig. A.2.1(a): pressure distribution at 6 degrees of AOA

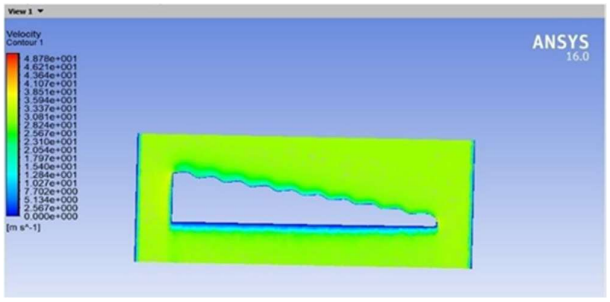

Fig. A.2.1(b): flow visualization at 6 degrees of AOA

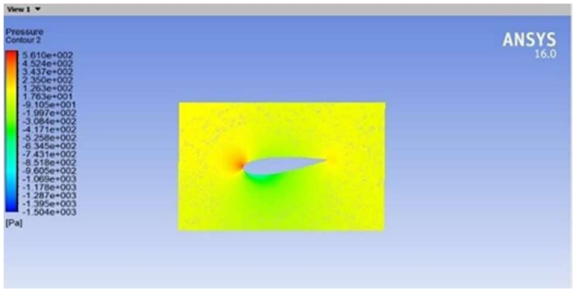

Fig.A.2.1(c): velocity distribution at 6 degrees of AOA

A.2.2 AT AOA 12 DEGREE:

At angle of attack 12 degree in the wavy wing design. The characteristic of flow over the entire wing span. However, observed the tubercle performance of the wing by the following figure. A flow visualization, pressure and velocity distribution of a semi wingspan (Fig A.2.2.a-b-c).

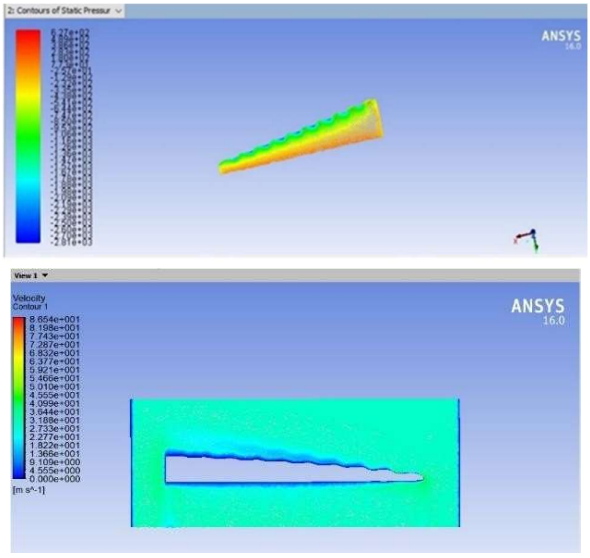

Fig. A.2.2(a): pressure distribution at 12 degree of AOA

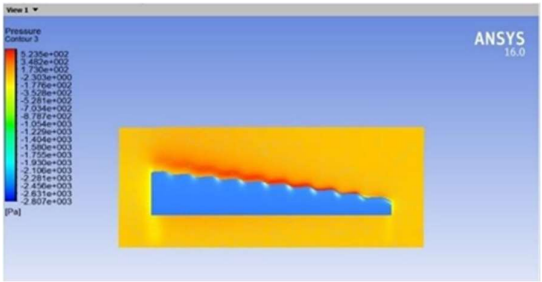

Fig. A.2.2(b): flow visualization at 12 degree of AOA

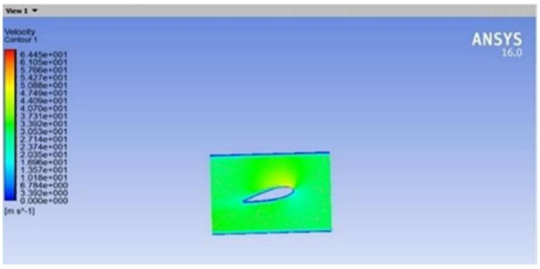

Fig.A.2.2(c): velocity distribution at 12 degree of AOA

A.2.3 AT AOA 18 DEGREE:

At angle of attack 18 degree in the wavy wing. The characteristic of flow over the entire wing span. However, observed the tubercle performance of the wing by the following figure. A flow visualization, pressure and velocity distribution of a semi wingspan (Fig A.2.3.a-b-c).

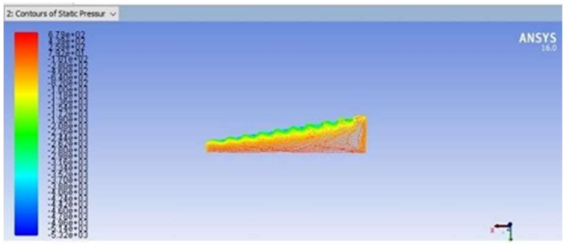

Fig. A.2.3(a): pressure distribution at 18 degrees of AOA

Fig. A.2.3(b): flow visualization at 18 degrees of AOA

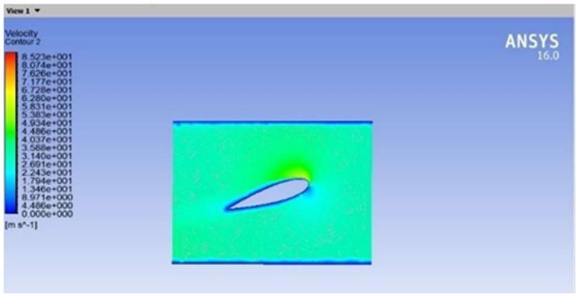

Fig. A.2.3(c): velocity distribution at 18 degrees of AOA

A.3 3/4th Distance of Wavy Taper Semi Wing:

A.3.1 AT AOA 6 DEGREE:

At angle of attack 6 degree in the wavy wing. The characteristic of flow over the entire wing span. However, observed the tubercle performance of the wing by the following figure. A flow visualization, pressure and velocity distribution of a semi wingspan (Fig A.3.1.a-b-c).

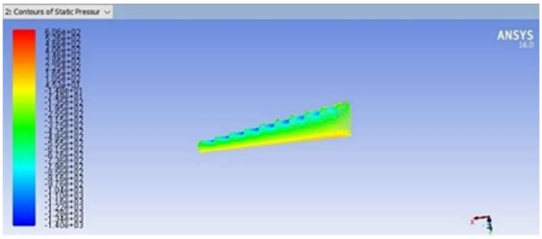

Fig. A.3.1(a): pressure distribution at 6 degrees of AOA

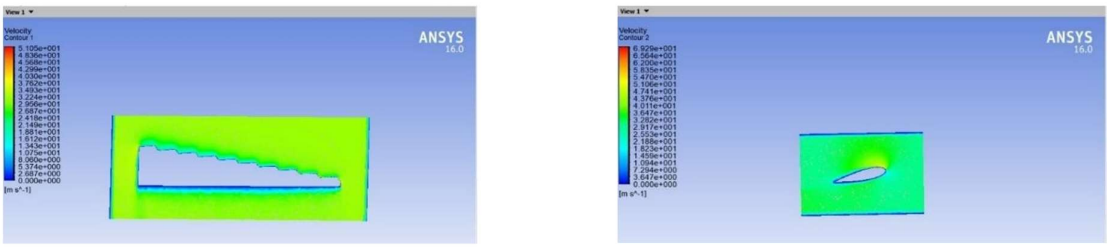

Fig. A.3.1(b): flow visualization at 6 degrees ofAOA

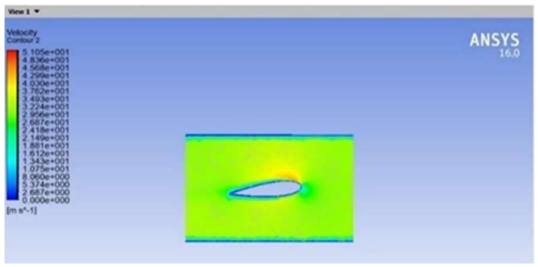

Fig. A.3.1(c): velocity distribution at 6 degrees of AOA

A.3.2 AT AOA 12 DEGREE:

At angle of attack 12 degree in the wavy wing. The characteristic of flow over the entire wing span. However, observed the tubercle performance of the wing by the following figure. A flow visualization, pressure and velocity distribution of a semi wingspan (Fig A.3.2.a-b-c).

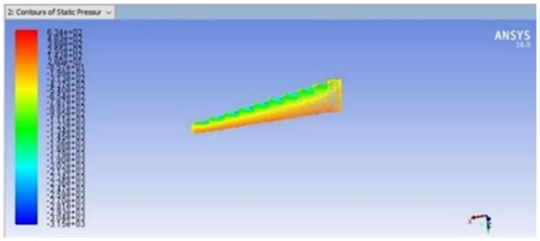

Fig. A.3.2(a): pressure distribution at 12 degree of AOA

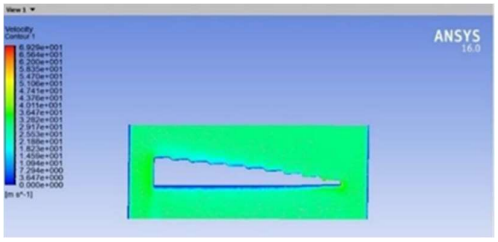

Fig. A.3.2(b): flow visualization at 12 degree of AOA

Fig. A.3.2(c): velocity distribution at 12 degrees of AOA

A.3.3 AT AOA 18 2DEGREE:

At 18 degrees of Angle of attack in the wavy wing. The characteristic of flow over the entire wing span. However, observed the tubercle performance of the wing by the following figure. A flow visualization, pressure and velocity distribution of a semi wingspan (Fig A.3.3.a-b-c).

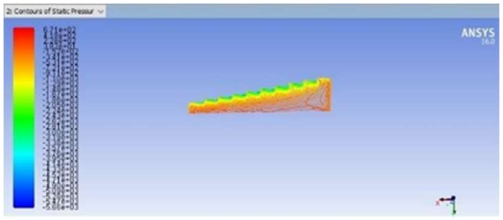

Fig A.3.3(A)pressure distribution at 18 degrees of AOA

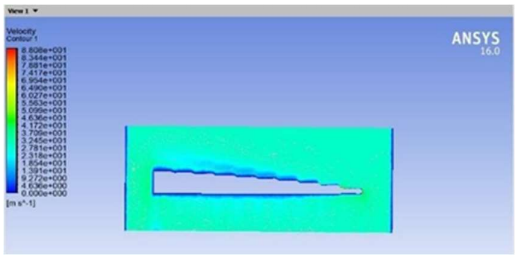

Fig A.3.3(b): flow visualization at 18 degree of AOA

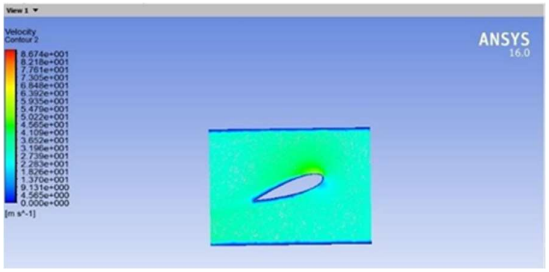

Fig. A.3.3(c): velocity distribution at 18 degrees of AOA

IV RESULTS:

A.1 Lift and Drag Results:

As results of aerodynamic performance and these design perform the maximum lift co-efficient when compared to smooth wing configuration.

A.2 Normal Taper Wing Performance at velocity 30.6m/S:

A.2.1 AT AOA 6 DEGREE:

The three-dimensional wing effects on normal taper wing, at velocity 30.6m/s. Calculate the co-efficient of lift and co-efficient of drag in graph form at angle of attack 6 degree.
(Graph.A.2.1. a-b)

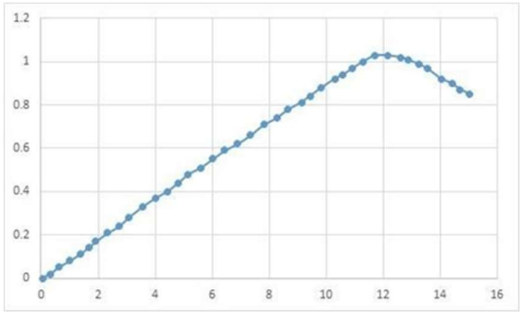

Angle of Attack (degree)

Graph.A.2.2(a): Co-efficient of lift at 12 degrees of AOA

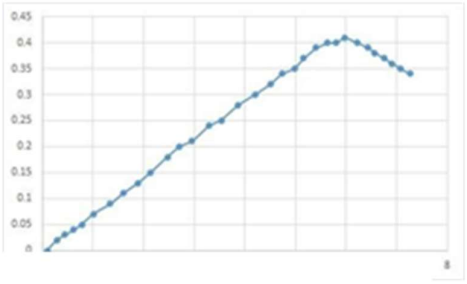

G Angle of Attack (degree)

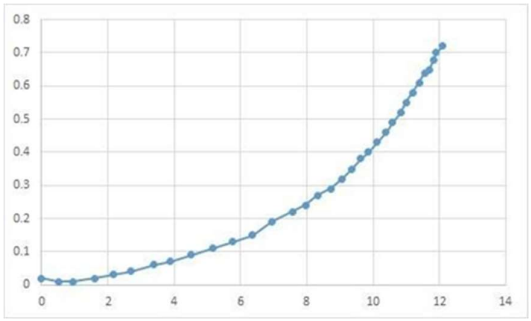

Angle of Attack (degree)

Graph.A.2.2(b): Co-efficient of drag at 12 degrees of AOA

A.2.3 AT AOA 18 DEGREE:

The three-dimensional wing effects on normal taper wing, at velocity 30.6m/s. Calculate the co-efficient of lift and co-efficient of drag in graph form at angle of attack 18 degree. (Graph.6.2.3. a-b)

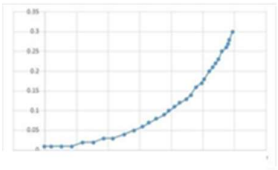

Graph A.2.1(b): Co-efficient of drag at 6 degrees of AOA

A.2.2 AT AOA 12 DEGREE:

The three-dimensional wing effects on normal taper wing, at velocity 30.6m/s. Calculate the co-efficient of lift and co-efficient of drag in graph form at angle of attack 12 degree. (Graph.A.2.2. a-b)

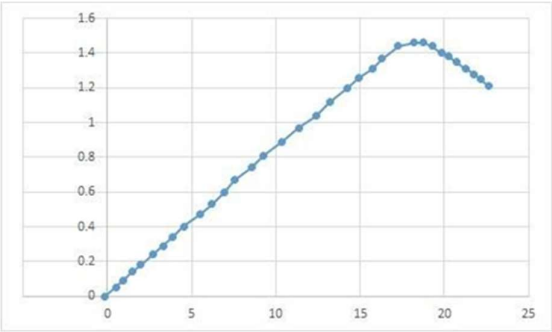

Angle of Attack (degree)

Graph.A.2.3(a): Co-efficient of lift at 18 degrees of AOA

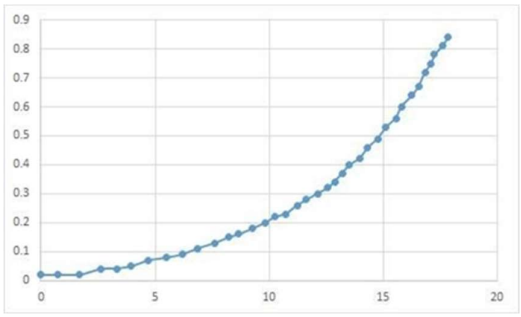

Angle of Attack (degree)

Graph.A.2.3(b): Co-efficient of drag at 18 degrees of AOA

A.3 Wavy Leading Edge Performance at Velocity 30.6 M/S in Half Of The Distance Of Wavy Wing:

A.3.1 AT AOA 6 DEGREE:

The half of the distance of three- dimensional wavy wing in leading edge performance, at velocity 30.6 m/s. Calculate the co- efficient of lift and co-efficient of drag in graph form at angle of attack 6 degree.

(Graph.A.3.1. a-b)

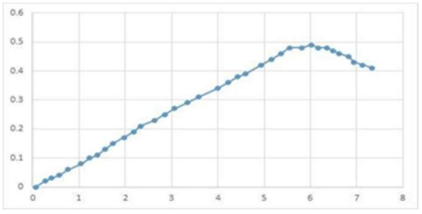

Angle of Attack (degree)

Graph.A.3.1(a): Co-efficient of lift at 18 degree of AOA

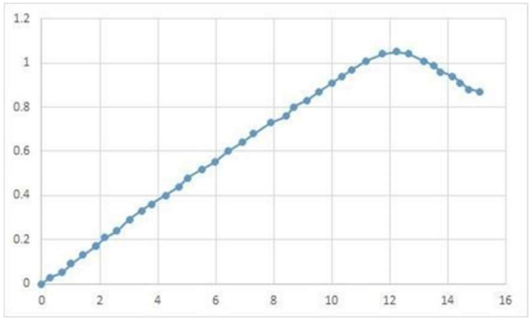

Angle of Attack (degree)

Graph.A.3.1(b): Co-efficient of drag at 6 degrees of AOA

A.3.2 AT AOA 12 DEGREE:

The half of thedistance of three- dimensional wavy wing in leading edge performance, at velocity 30.6 m/s. Calculate the co- efficient of lift and co-efficient of drag in graph form at angle of attack 12 degree

(Graph.A.3.2. a-b)

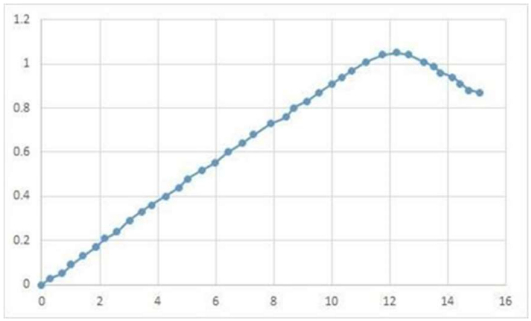

Angle of Attack (degree)

Graph.A.3.2(a): Co-efficient of lift at 12 degrees of AOA

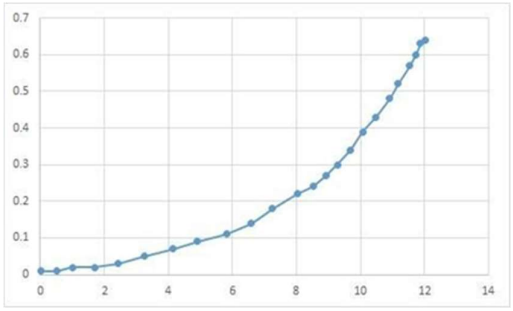

Angle of Attack (degree)

Graph.A.3.2(a): Co-efficient of drag at 12 degrees of AOA

A.3.3 AT AOA 18 DEGREE:

The half of the distance of three- dimensional wavy wing in leading edge performance, at velocity 30.6 m/s. Calculate the co- efficient of lift and co-efficient of drag in graph form at angle of attack 18 degree.

(Graph.A.3.3. a-b)

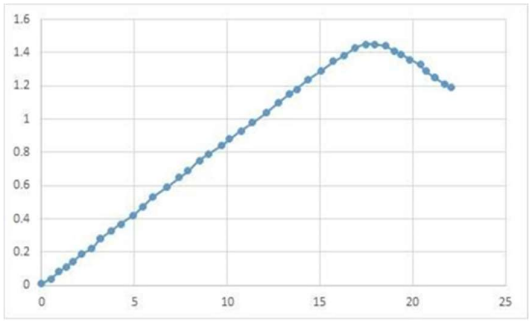

Angle of Attack (degree)

Graph.A.3.3(a): Co-efficient of lift at 18 degrees of AOA

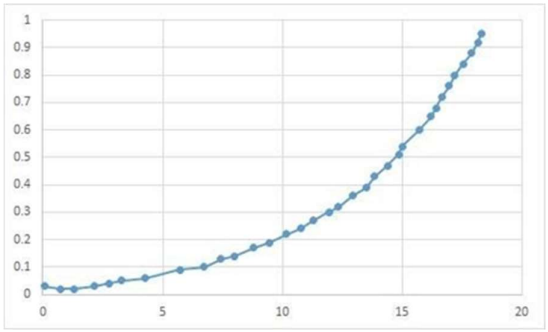

Angle of Attack (degree)

Graph.A.3.3(b): Co-efficient of lift at 18 degrees of AOA

A.4wavy Leading Edge Performance at Velocity30.6 M/S In ¾Th of The Distance Of Wavy Wing:

A.4.1 AT AOA 6 DEGREE:

The 3/4th of the distance of three- dimensional wavy wing in leading edge performance, at velocity 30.6 m/s. Calculate the co- efficient of lift and co-efficient of drag in graph form at angle of attack 6 degree. (Graph.A.4.1. a- b)

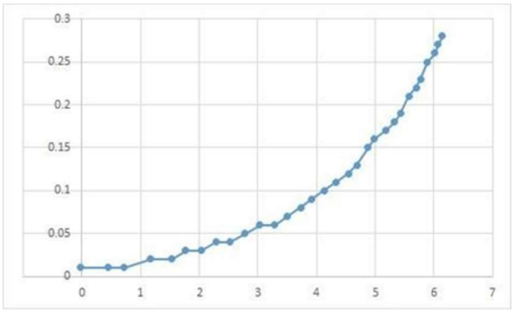

Angle of Attack (degree)

Graph.A.4.1(b): Co-efficient of lift at 6 degrees of AOA

A.4.2 AT AOA 12 DEGREE:

The 3/4th of the distance of three- dimensional wavy wing in leading edge performance, at velocity 30.6 m/s. Calculate the co- efficient of lift and co-efficient of drag in graph form 12 degree of AOA.

h.A.4.2. a-b)

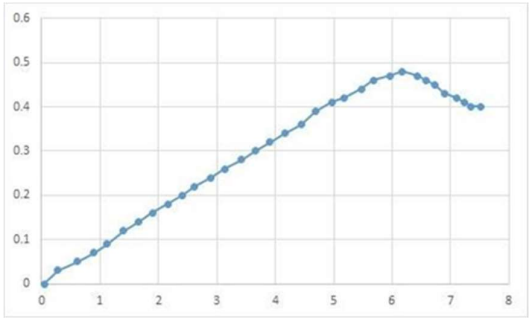

Angle of Attack (degree)

Graph.A.4.1(a): Co-efficient of lift at 6 degrees of AOA

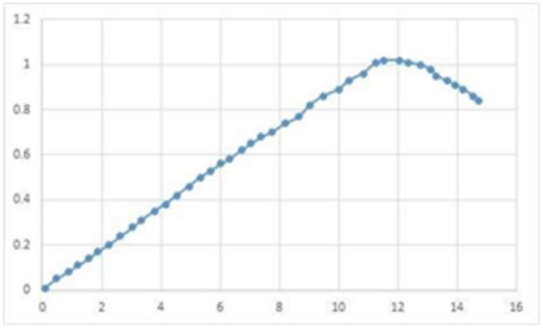

Angle of Attack (degree)

Graph.A.4.2(a): Co-efficient of lift at 12 degree

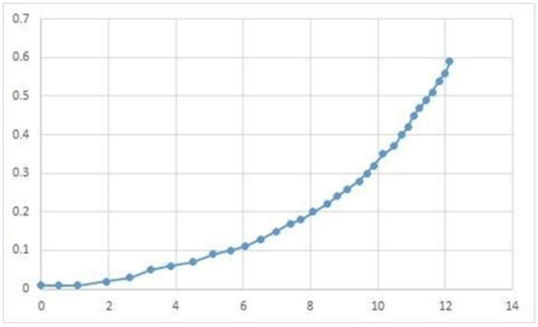

Angle of Attack (degree)

Graph.A.4.2(b): Co-efficient of lift at 12 degrees of AOA

A.4.3 AT AOA 18 DEGREE:

The 3/4th of the distance of three- dimensional wavy wing in leading edge performance, at velocity 30.6 m/s. Calculate the co- efficient of lift and co-efficient of drag in graph form 18 degree of AOA. (Graph.A.4.3. a-b)

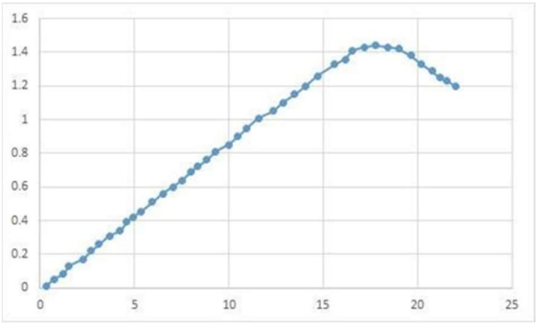

Angle of Attack (degree)

Graph.A.4.3(a): Co-efficient of lift at 18 degree of AOA

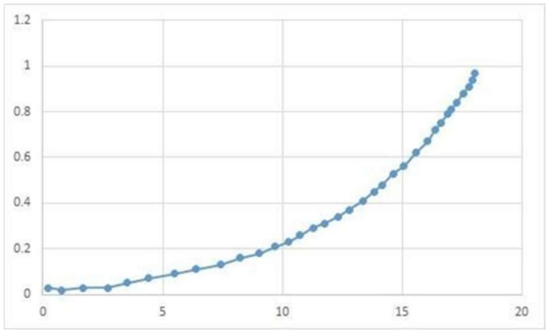

Angle of Attack (degree)

Graph.A.4.3(b): Co-efficient of lift at 18 degrees of AOA.

6.5 COMPARING RESULTS:

Table.6.5Comparing Result

SL.NO	SEMI WING	α (AOA) degree	Cl(N)	Cd(N)
1	Normaltaper wing	6	22.1346	10.5557
		12	45.7440	26.5090
		18	63.8878	54.9649
2	Half ofthe distanceof wavy wing	6	23.1083	11.0516
		12	45.7120	28.9922
		18	68.4435	57.9200
3	$3/4^{th}$ distanceof thewavy wing	6	23.1490	10.9775
		12	46.0772	29.4974
		18	69.0638	58.7255

V DISCUSSION AND CONCLUSION

The lift, drag force, flow visualization consequence shows that the three dimensional impacts on the wavy wing. As results of the wavy wing design achieves lower maximum lift co-efficient and then compared to smooth wing. The wavy configuration gives increases in the flow separation and area along the span wise and chord wise. As results of the separation of flow is caused by wavy. The wavy taper wing design gives lower value of lift co-efficient and then not showing the aerodynamic deterioration at low angle of attack.

In maximum lift co-efficient, consider the smooth and wavy wings the (Fig 3(a) and 3(b)) at 6 degree of AOA. Finally compare the two semi wing at same AOA and they obtaining half of

the distance of wavy wing occurred high lift co- efficient compared to the smooth wing (Graph A.2.1.a-b, and Graph A.3.1.a-b). Again comparing the result but these semi wing at AOA 12 and 18 degrees Also, they obtaining half of the distance of wavy wing occurred high lift co-efficient compared to the smooth wing at 12 and 18 degrees of AOA (Graph A.2.2a-b, A.2.3. a-b and Graph A.3.2a-b, A.3.3. a-b). The smooth wing and half of

the distance of wavy wing is compared to the 3/4th distance of wavy wing. It shows that 3/4th of the wavy wing reach the highest values lift co-efficient and also the same velocity condition and same degree of AOA (Graph A.4.1.a-b, A.4.2a-b, A.4.3. a-b). The 3/4th of wavy taper wing model to be stupendous wing design for aircraft design at low velocity. The (Fig 3(b) and Graph A.4.1.a-b, A.4.2a-b,A.4.3.a-b) show improvement in CLmax value is higher compared to the smooth and half of the wavy wing configurations at low velocity 30.6m/s respectively.

VI REFERENCE

1. Miklosovic, M.M., Howle, D.S., Murray, F.E. Leading edge tubercles lag stall on Humpback whale flippers, Physics of Fluids, Vol.16,No.5,pp.39-42,2004, L.E. e Fish.
2. Miklosovic, M.M. e Howle, D.S., Murray,L.E. Experimental evaluation of sinusoidal leading edges, Journal of Aircraft , Vol.44, No. 4,pp. 1404-1407,2007.
3. Johari H, Henoch, Levshin , C.,Custodio D., A. Effects of leading-edge protuberances on airfoil performance AIAA J 45:2634-42.2007.
4. Custodio,D. Master of sciences in mechanical engineering, The Effect of Humpback whale like leading edge protuberances on hydrofoil performance, Worcester polytechnic institute,2007.
5. Stanway, Master of science in ocean Engineering, M. J. Hydrodynamic effects of leading edge tubercles on control surfaces and in flapping foil propulsion. Massachusetts institute of technology,2008.
6. Hansen K.L.; Dally B.B, Kelso R.M.. Proceedings of the 17th Australasian Fluid Mechanics conference. Auakland, New zealand 2010. An investigation of three- dimensional effects on the performance of tubercles at low Reynolds number.
7. Custodio, D.; Johari, H. Henoch, C. Proceedings of the 50th AIAA Aerospace science Metting. Nashville, Tennessee: AIAA paper 2012-0054,2012. Aerodynamic characteristics of finite span wings with leading edge protuberances.
8. New, T.H; Toh, J. W.A.; Wei, Z.; Cui, Y D.Effects of leading- edge tubercles on swept tapered wing flow characteristics. 11th European fluid mechanics conference, At Seville, Spain
9. Bolzon, M. D; M; Arjomandi, M. Kelso, R. The effects of tubercles on swept wing performance at low angles of attack. 19th Australasian Fluid Mechanics Conference. Melbourne, Australia. Conference Paper: pp. 8- 11, 2014.
10. De Paula, A. A.; Padilha, B. R. and Meneghini, J. Mattos B. S.; The Airfoil Thickness Effect on Wavy Leading Edge Performance, 54th AIAA Aerospace Sciences Meeting, AIAA Paper 2016-1306, 2016.

11. De Paula A. A. The airfoil thickness effects on wavy leading edge phenomena at low Reynolds number regime, Doctoral Thesis in Mechanical Engineering, University of Sao Paulo, 2016.
12. Abrantes, , A. A. R. De Paula, A. T. T.
S. Curuz A. The Wing Three-Dimensional Effects on Wavy Leading Edge Performance, AIAA Aviation, 2017.
13. Wei, Z., Mew, T,H., Howle, Y. D. Aerodynamics performance and surface flow structures of leading-edge tubercled tapered swpt- back wings, Journal of Aircraft, Vol. 56, No. 1, 2018.